Bulletin of the Seismological Society of America, Vol. 94, No. 6, pp. 2265–2279, December 2004

# Reference Events for Regional Seismic Phases at IMS Stations in China

by Felix Waldhauser and Paul G. Richards

Abstract Seismic-event location within the context of monitoring the Comprehensive Nuclear-Test-Ban Treaty entails *a priori* knowledge of the travel time of seismic phases for a given source to stations of the International Monitoring System (IMS). Such travel-time information (or ground truth, GT) is provided empirically by seismic reference events, events that have well-determined hypocenter locations (epicenters typically known to $\pm 5$ km with high confidence) and origin times. In this study we present new reference events for the calibration of six seismic stations of the IMS in China, a region with high seismic activity. We use the *Annual Bulletin of Chinese Earthquakes*, which lists about 1000 earthquakes in and near China each year with consistent phase picks at regional stations, to determine precise relative earthquake locations from double-difference cluster analysis. The resulting high-resolution image of active faulting at seismogenic depths in areas of dense seismicity is correlated with the tectonic structure derived from mapped fault information at the surface to validate the absolute locations. We generated 59 reference events with $M \geq 3.5$, distributed in six clusters in central and eastern China, and recorded by at least one of the six IMS stations. The scatter in relative travel-time residuals is reduced from 1.28 sec before to 0.61 sec after relocation, consistent with the relocated positions of the events. The degree of correlation between seismicity structure and well-characterized fault data indicates that, in four clusters, the locations of the new reference events are accurate to within 5 km (GT5), and in two clusters within 10 km (GT10).

## Introduction

Effective monitoring of compliance with the Comprehensive Nuclear-Test-Ban Treaty (CTBT) requires prompt and accurate characterization of about 100 seismic events per day. Such characterization entails the need for accurate location estimates, which in turn requires knowledge of the travel time of seismic phases such as *Pg*, *Pn*, teleseismic *P*, and their *S*-wave analogs for a given source-station configuration. It has become conventional to describe these travel times in terms of Source Specific Station Corrections (SSSCs), which are added to the travel times predicted by a standard travel-time model (usually taken as IASP91; see Kennett and Engdahl, 1991) to obtain travel times at a particular station as a function of distance, azimuth, and depth. When implemented at the International Data Centre (IDC) in Vienna, for stations of the International Monitoring System (IMS), SSSCs are expected to improve event locations by removing location bias resulting from unmodeled velocity structure between source and receiver. With the increasing amount and quality of seismic data collected by the IMS, unmodeled velocity structure remains the main cause of significant errors and uncertainties in the location of seismic events for monitoring purposes. This is especially true for regional signals, whose travel time can be significantly different (fast or slow) in comparison with the predictions of travel-time models that represent global averages.

In recent years, SSSCs have been developed by using seismic-velocity models of the crust and upper mantle for the region surrounding an IMS station (e.g., Yang *et al.*, 2001; Murphy *et al.*, 2002; Ritzwoller *et al.*, 2003). These models are generally based on active or passive seismic data, or a combination of both, and travel times have been computed through these models from a station to a set of surface grid points within 20° distance. A critical step in producing SSSCs is the process by which these correction surfaces are validated against independent data, such as reference events. Reference events are seismic events whose location and origin time are known independently of the monitoring network. Their location uncertainty within the 90% confidence level is generally referred to as the ground-truth level of an event, GT*x*, where *x* specifies the epicenter location accuracy in kilometers (i.e., true epicenter lies within *x* kilometers of the estimated epicenter) (Bondár *et al.*, 2001). GT0 reference events, for example, have epicenters and origin times known to within 100 m and 0.1 sec, respectively, and are typically obtained from peaceful nuclear or chemical explosions (e.g., Sultanov *et al.*, 1999). Because the global distribution of

man-made sources with well-known source parameters is sparse, data from moderate-size earthquakes must also be used. The location of earthquakes, however, is generally much less well known. Typically, events of GT5 quality or better are obtained when the earthquake occurred within a local network. A significant effort is necessary to turn earthquake locations into reference events of GT5 quality when they occur within regional networks.

In this study we follow an integrated approach to generating reference events from regional network data for IMS station calibration in central and eastern China. The complex tectonics in this region are expressed by quite high but diffuse seismicity. We analyze more than 11,000 events in the *Annual Bulletin of Chinese Earthquakes* (ABCE) from 1985 to 1999 for their potential use as reference events. Many of these events are recorded at ABCE stations that are close to or co-locate with the planned IMS stations (Table 1). We determine 59 reference events at the GT5 and GT10 levels in central and eastern China by combining precise relative-event relocations obtained from cluster analysis of ABCE data with a database of mapped fault information at the surface. While the motivation of this work was within the context of CTBT monitoring, the approach outlined here may be useful for other purposes, for example, to image faults at seismogenic depths over large areas for seismic-hazard investigations. For such studies, however, the ABCE data need to be combined with provincial- and local-network data across China.

## ABCE Data and Double-Difference Cluster Analysis

An electronic version of the ABCE (z-files, included in the *IASPEI International Handbook of Earthquake and Engineering*, Part B, 2003) includes about 14,000 events in and near China with magnitudes up to *M* 6.8 that occurred between 1985 and 1999, with more than 10,000 events located in mainland China (Fig. 1). *P*- and *S*-phase picks are available for 170 regional stations in and near China. These picks are remarkably consistent as noted by Hearn and Ni (2001) and demonstrated by the analysis of travel-time residuals below. About 36,000 *P*-phase picks, selected from 11,500 events recorded at ABCE stations BJI, HLR, KMI, LZH, SSE, and XAN, and located within 20° of each station, are analyzed for their accuracy. These six stations are at or close to the designated sites of IMS stations in China (Table 1). A total of 96% of the ABCE *Pn*-phase picks are reported to a tenth of a second (Fig. 2a). Locations of 43% of the events are rounded to the nearest tenth of a degree, introducing (presumably randomly distributed) location uncertainties of up to 5 km (Fig. 2b). Depths for about 50% of the events appear to be fixed at 10, 15, or 33 km (Fig. 2c).

In addition to an electronic ABCE, we have access to a printed version of the ABCE for events that occurred in 1985 and 1986, and in the years 1991–1995. The printed ABCE reports earthquake locations to the nearest hundredth of a degree, and they appear to be a revised version of the electronic ABCE. Comparison between event locations on mainland China in the printed ABCE and the corresponding events in the electronic ABCE indicates a mean-event mislocation of about 11 km in both horizontal directions. Comparison of the electronic ABCE with data from a local network in the Sichuan/Yunnan Province (Z. Yang, personal comm.) indicates similar differences, but individual errors may be larger in some areas.

Table 1
IMS (ABCE) Stations Considered in This Study

| Station | Latitude | Longitude | Network |
|---|---|---|---|
| PS12 (HLR) | 49.27 | 119.74 | Primary |
| PS13 (LZH) | 36.09 | 103.84 | Primary |
| AS20 (BJI) | 40.02 | 116.17 | Auxiliary |
| AS21 (KMI) | 25.15 | 102.75 | Auxiliary |
| AS22 (SSE) | 31.10 | 121.19 | Auxiliary |
| AS23 (XAN) | 34.04 | 108.92 | Auxiliary |

Owing to uncertainties of this order in ABCE locations, we cannot extract high-quality reference events directly from the catalog, but accurate event locations may be determined by relocating the events. Relocation of the ABCE data for the purpose of obtaining reference events is problematic, however, because of the sparse distribution of available stations for most of the events. None of the events in the ABCE has the potential to achieve GT5 status at the 95% confidence level on the basis of the seismic-network criteria put forward by Bondár *et al.* (2004). These criteria require at least 10 stations within 250 km with an azimuthal gap less than 110°, a secondary azimuthal gap less than 160°, and at least one station within 30 km from the epicenter. We can turn instead to relative-location methods such as the double-difference technique of Waldhauser and Ellsworth (2000) to reduce the effect of model errors, and then use near-surface information to constrain the absolute locations.

The fundamental equation of the double-difference algorithm relates the differences between the observed and predicted phase travel-time difference for pairs of earthquakes observed at common stations to changes in the vector connecting their hypocenters. By choosing only relative phase travel times for events that are close together (i.e., closer than the scale length of the surrounding velocity heterogeneity), wave paths outside the source region are similar enough so that common-mode travel-time errors are canceled for each linked pair of events. It is then possible to obtain high-resolution hypocenter locations over large areas without the use of station corrections. This approach is extremely useful in our search for potential reference events across China, as it allows us to efficiently relocate dense seismicity across large areas. In some of the clusters investigated in this study the seismicity spreads over more than 100 km, in which case we linked events over short distances (typically less than 10 km) to build a chain of links that connect events across the entire cluster. Other multiple-event location algorithms such as JHD (Douglas, 1967) or HDC

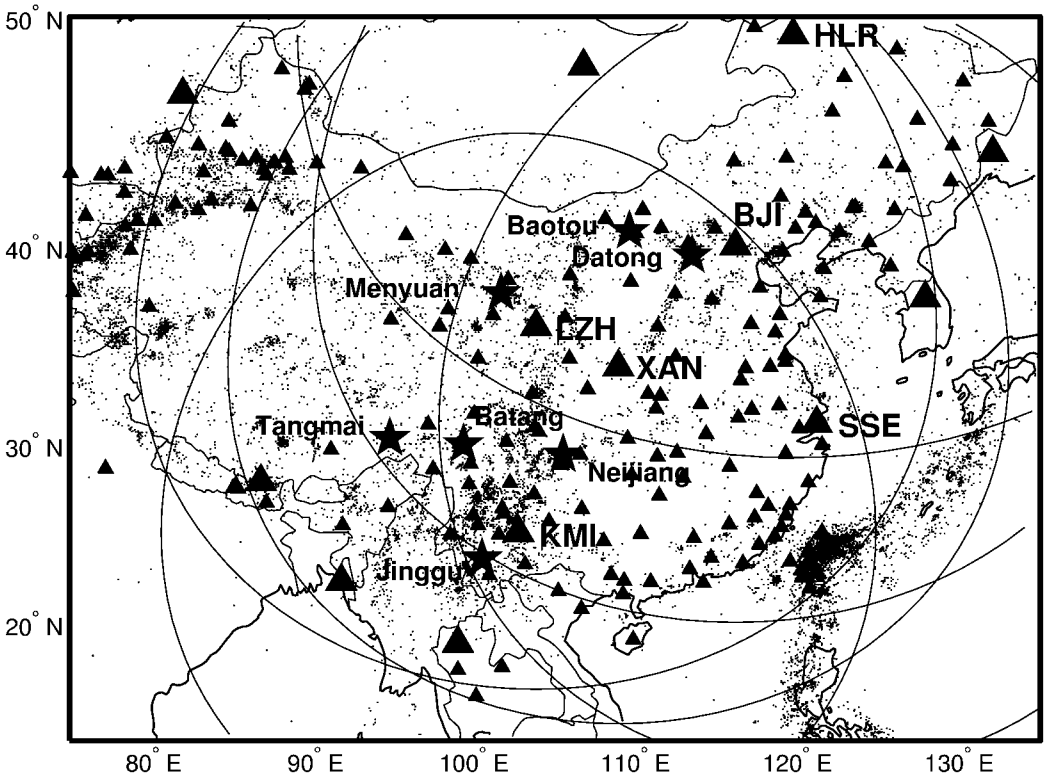


Figure 1. Events (dots) and Chinese stations (small triangles) listed in the ABCE. IMS stations (large triangles) are indicated, and the ones discussed in this study are labeled. Stars indicate locations at which reference events are obtained. Circles denote areas out to 20° from each of the labeled IMS stations.

(Jordan and Sverdrup, 1981) employ station corrections that are fixed for a particular cluster of events, thus limiting the spatial area within which events can be relocated.

The presence of severely mislocated events in the ABCE can hamper the inversion, because the linearization of the nonlinear double-difference location problem (which solves for adjustments to initial locations) requires the initial locations to be close to their true value. To stabilize the inversion, we search for clusters of well-linked event pairs (at least 10 stations), and iteratively solve the system of weighted double-difference equations by means of least squares using the program *hypoDD* (Waldhauser, 2001). Convergence to a stable solution is greatly helped by the high quality of the ABCE phase picks, which have little contamination by outliers. A search of the ABCE for clusters of events that are most suitable for double-difference relocation in terms of network geometry and event density resulted initially in 36 clusters, ranging in size between 20 and 344 earthquakes. This analysis was done by searching about 460,000 *P*- and *S*-phase picks. For the 36 clusters, *P*- and *S*-phase pairs at common stations out to 2000 km distance were formed. Regional 1D layered velocity models were used to predict the travel-time differences and partial derivatives. These models were adapted from the models used for routine locations at Chinese provincial seismographic networks (Jih, 1998).

In many of the 36 clusters the high-resolution relocations reveal detailed structural information about the active faults on which they occur, such as dip and strike. It is possible to validate the absolute location accuracy of such an event cluster by comparing the relocated seismicity with independent surface information. Extremely detailed fault data for mainland China have been prepared by the U.S. Geological Survey (USGS Astrogeology Team, lead by Philip A. Davis), derived from volumes on the regional geology of Chinese provinces published by the Geological Publishing House (Beijing, 1984–1993). The Geographic Information System (GIS) database includes all fault lines, and additional fault parameters such as type of fault, age and name of fault, relative depth of the fault, how the existence of the fault was inferred, and the direction and amount of dip on the fault plane. These additional parameters, however, are not reported for all faults. Also, the location of the fault lines are subject to uncertainties owing to inconsistencies in the published maps and/or uncertainties related to the digitizing and GIS mapping process, according to the unpublished database documentation "Compilation of bedrock geology and structure databases of China, including relevant ancillary databases compiled by Los Alamos National Laboratory." In general the uncertainties range from a few hundreds of meters to a few kilometers in rare cases. Specifically, the deep faults in this study were drawn with very thick lines

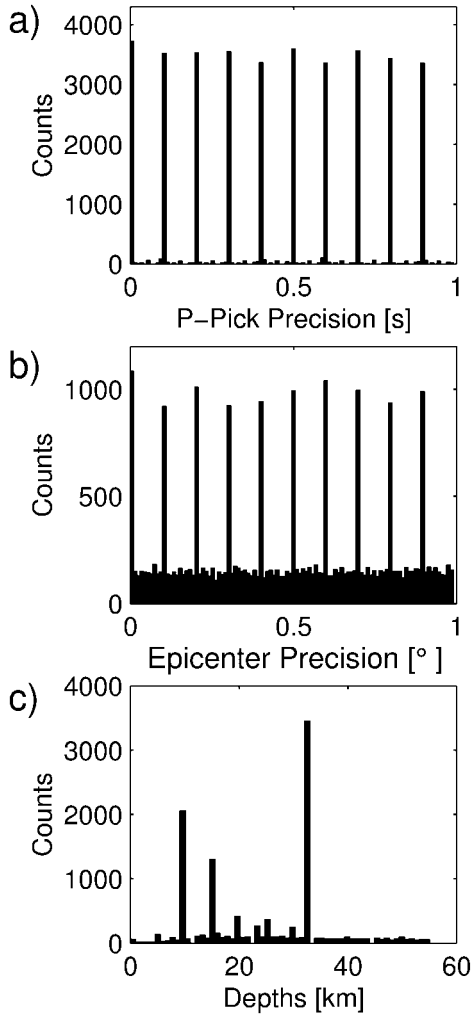


Figure 2. Reporting precision of (a) ABCE *P*-phase picks and (b) epicenter locations. In (a) the distribution is shown for fractions of seconds, in (b), fractions of degrees. (c) Distribution of event depths.

on the published Chinese maps, which translate to a possible maximum uncertainty of 0.5 km in the digital map provided by the USGS.

In order to extract potential reference events for the purpose of IMS station calibration from any of the 36 clusters, we have defined the following three criteria: The relocated seismicity

- includes events of $M \geq 3.5$ that have small relative-location errors and are recorded by at least one of the planned IMS stations (or a surrogate) within a 2000-km distance,
- indicates fault structure such as strike and dip,
- and correlates with nearby major deep-reaching faults or faulting patterns included in the Chinese fault database.

The 36 clusters are reviewed in terms of their location close to faults labeled as "deep reaching" in the database, or faults that have additional information to support their association with the seismic activity. In most of the 36 cases, no unique association with mapped surface traces is possible. Figure 3 shows two of such clusters in Guizhou Province and Sichuan Province. For the Guizhou cluster (Fig. 3a) the seismicity spreads over several faults, indicating that the events did not occur on a single fault, but rather on different adjacent faults. Only a few events appear to have occurred on a deep-reaching, right-lateral strike-slip fault (thick line in Fig. 3a), making a clear association difficult. Figure 3b shows a cluster of events that locates within an aseismic block bounded by deep-reaching faults to the southwest and the southeast, more than 40 km from any mapped surface trace. While it is possible that these locations are accurate to within a few kilometers, we cannot verify that accuracy with independent surface data, which our approach to build reference events requires.

Our detailed investigation of the 36 clusters resulted in a subset of 6 that has a positive correlation between the high-resolution seismic locations and available well-characterized fault data. These six clusters include a total of 262 events, located in central and eastern China in the provinces of Sichuan (near the cities of Neijiang and Batang), Shanxi (near Datong), Tibet (near Tangmai), Qinghai (near Menyuan), and Yunnan (near Jinggu) (Fig. 1). All six clusters include events with $M \geq 3.5$. (For the events we used whose magnitudes were not reported in the ABCE catalog, the large distances out to which these events were recorded indicate that they have magnitudes well above 3.5.)

## Generation of Reference Events

Events in the Neijiang cluster are used to demonstrate the improvement in event relocations over the ABCE locations. This cluster in Sichuan Province includes 61 events that were recorded at 31 stations between 1989 and 1999 (Fig. 4). The maximum separation between events that are linked together by common phase pairs is 10 km, while the cluster dimension is about 25 km. The largest azimuthal station gap is 40°, and the closest station is 120 km away (Table 2). Table 3 lists the regional (Sichuan/Yunnan) velocity model used for relocation. Figure 5 compares the double-difference epicenter locations with the locations listed in the ABCE. The double-difference locations indicate a much tighter distribution compared to the ABCE, and concentrate near a deep, north-dipping reverse fault mapped at the surface by Chinese scientists (thick fault trace in Fig. 5). Shifts between ABCE and double-difference locations range from 0.5 to 40 km, with a mean of about 13 km. Shifts in origin times range from $-4.9$ to 4.3 sec, with a mean of $-0.08$ sec and a standard deviation of about 2 sec. The root mean square (rms) residual after relocation is 0.7 sec, down 72% from the initial value. A bootstrap analysis of the remaining differential time residuals (see Waldhauser and Ellsworth, 2000, for details) has been performed to assess the relative-location uncertainty at the 90% confidence level. The rms values for semimajor and semiminor axes are 1.5 and 0.85

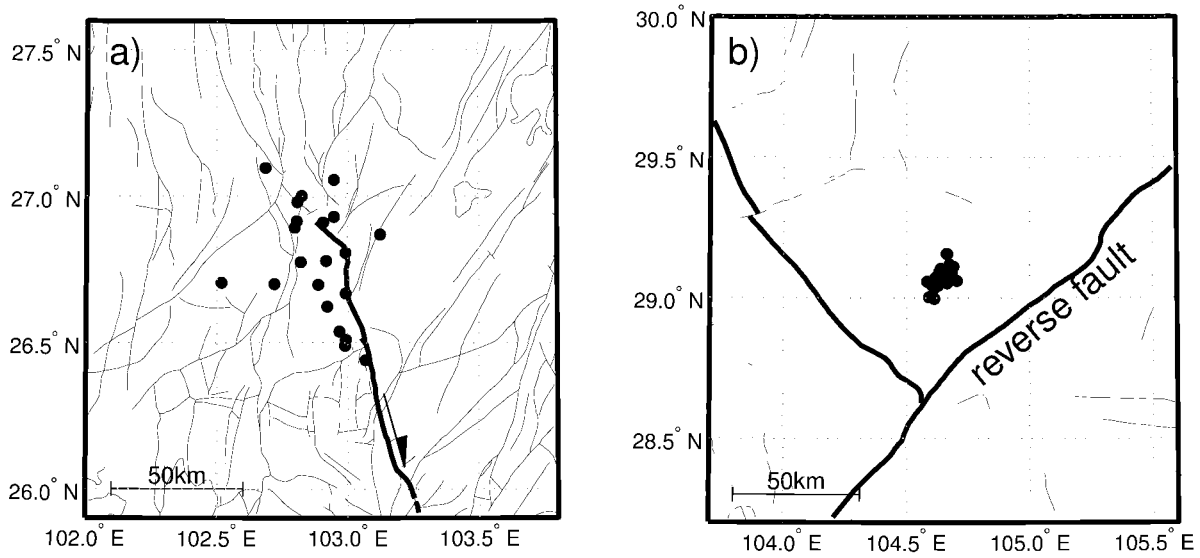


Figure 3. Two examples where no unique association of the relocated seismicity with an active fault is possible. (a) Twenty-one events, which occurred between 1987 and 1998, do not appear to occur on a single deep fault, but rather on a set of adjacent smaller faults. (b) Thirty-eight events, which occurred between 1985 and 1996, are located more than 40 km from the nearest mapped fault.

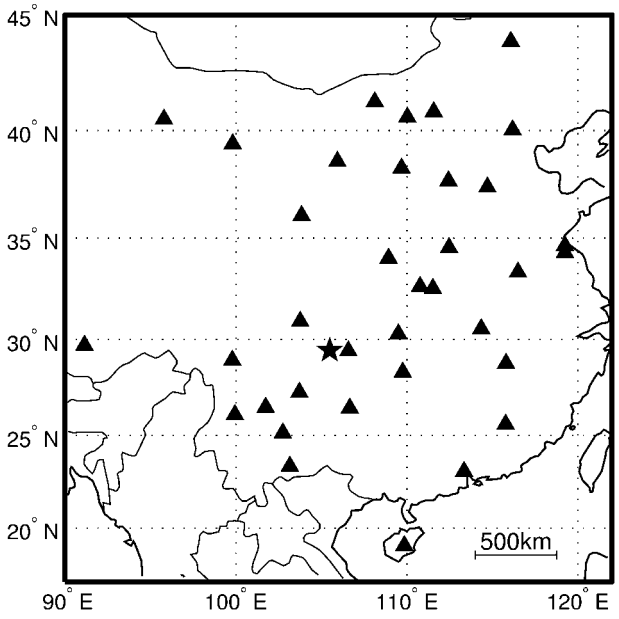


Figure 4. Stations (triangles) that recorded the 61 events near Neijiang, Sichuan Province. Star indicates the location of the cluster.

km, respectively, and 1.5 km for errors in depths, for all 61 events.

Figures 6a–f show the relocation results for the six clusters, both in map view and fault perpendicular cross section (along AA′), superimposed on the near-surface information from the Chinese fault database. Relative-location errors from the bootstrap analysis are indicated in map view as ellipses and in the fault-perpendicular cross section as crosses. Station distributions for each cluster are indicated in Table 2, velocity models upon which the models used for relocation are based on Table 3 and final hypocentral parameters for the selected reference events in Table 4. The velocity models in Table 3 were modified by introducing additional thinner layering across strong velocity contrasts. Fault traces in map views of Figure 6 are represented by lines, with thick lines indicating deep-reaching faults. Additional structural information is included where available. Fault traces in cross sections of Figure 6 are represented by triangles as the projection of the main fault onto the cross sections.

Although the double-difference algorithm is somewhat sensitive to absolute locations through a chosen model (see Waldhauser and Ellsworth, 2000), we have fixed, for all six clusters, the absolute centroid location (epicenter and depth) of the double-difference solutions at the position of the centroid derived from the events in the electronic ABCE or the printed ABCE. A comparison between the two catalogs for events in 1985 and 1986, and in the years 1991–1995 (years for which the printed ABCE is available), shows that the difference in centroid location is less than 4 km for the clusters near Neijiang, Datong, Batang, and Tangmai. For the Neijiang cluster, for example, it is about 3 km for the 25 events that are included in both catalogs (see stars in Fig. 5a). Even though it appears that the printed ABCE is a revised version of the electronic ABCE, we use the centroid location from the events in the electronic ABCE for the four clusters because the electronic ABCE includes all events in comparison to the printed ABCE's limited number of years. Furthermore, the differences in hypocentroid locations are smaller than the GT5 level we aim to achieve. For the two

Table 2
Station Distributions

| | Neijiang | Datong | Batang | Tangmai | Menyuan | Jinggu |
|---|---|---|---|---|---|---|
| Number of stations | 36 | 64 | 67 | 58 | 17 | 13 |
| Distance to nearest station (km) | 120.5 | 210.4 | 125.5 | 274.9 | 86.3 | 191.4 |
| Max. azimuth gap (°) | 40.2 | 70.7 | 42.9 | 48.3 | 71.1 | 135.5 |

Table 3
Regional Velocity Models: Depth to Top of Layer (in km); *P*-velocity, $V_p$, (in km/s)

| Sichuan/Yunnan* | | Tibet† | | Gansu-Qinghai† | | NE China, A† | | IASP91 | |
|---|---|---|---|---|---|---|---|---|---|
| Depth | $V_p$ | Depth | $V_p$ | Depth | $V_p$ | Depth | $V_p$ | Depth | $V_p$ |
| 00.0 | 5.00 | 00.0 | 5.55 | 00.0 | 6.10 | 00.0 | 5.95 | 00.0 | 5.80 |
| 07.5 | 5.48 | 15.8 | 6.25 | 22.0 | 6.47 | 17.0 | 6.50 | 20.0 | 6.50 |
| 16.0 | 5.93 | 69.3 | 7.97 | 51.5 | 8.17 | 33.0 | 7.80 | 35.0 | 8.04 |
| 20.0 | 6.43 | | | | | | | | |
| 30.0 | 6.60 | | | | | | | | |
| 50.0 | 8.30 | | | | | | | | |

*Z. Yang, personal comm.
†Jih (1988).

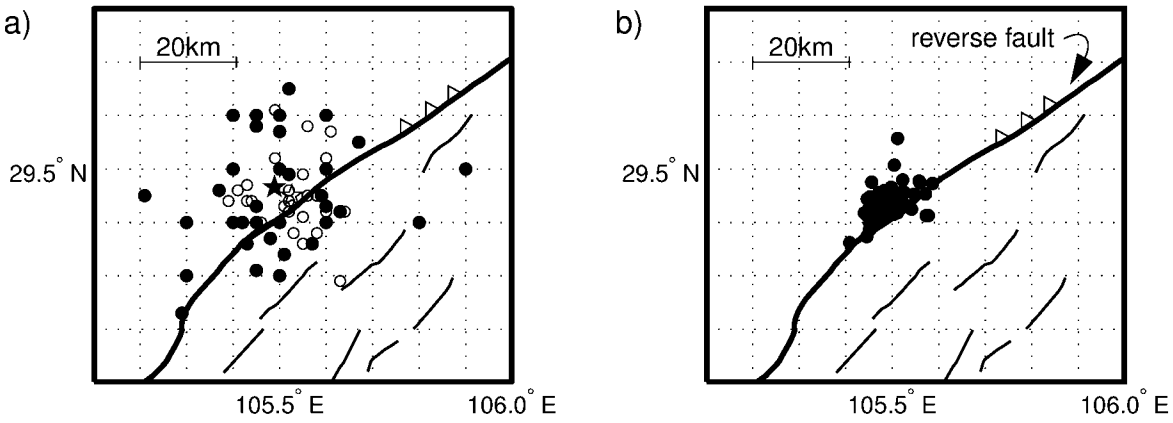


Figure 5. Map view of (a) ABCE locations and (b) double-difference locations. Solid circles in (a) indicate locations from the electronic ABCE, and open circles those from the printed ABCE. Solid and open stars represent the centroid of the electronic and printed ABCE locations, respectively. Lines indicate mapped surface traces of deep reverse faults.

clusters near Menyuan and Jinggu, however, the differences in cluster centroids derived from the electronic and the printed ABCE are larger than 5 km. The Menyuan cluster centroid as taken from the printed ABCE is about 0.05° to the north and 0.035° to the east from the one computed from the electronic ABCE. For the Jinggu cluster the shift is 0.01° and 0.09° to the south and east, respectively. For these two clusters we use the centroids from the printed ABCE, because of the significant deviation in centroid locations and the fact that most events in these two clusters are included in the printed ABCE. Note that in none of the six cases did we move the cluster of relocated events to line up with the surface trace of the fault. The fault information is considered independent data that are used to validate the absolute location of these clusters of reference events (as taken from the ABCE bulletins), and to investigate their level of accuracy in a tectonic context, discussed as follows.

The relocated seismicity in the Neijiang cluster (Fig. 6a) images a ~25-km-deep, about 10° northwest-dipping fault that correlates well with an isolated mapped surface trace described as a deep reverse and north-dipping fault in the fault database (thick line in map view in Fig. 6a). In cross section, the projection of this fault along line AA′ is indicated by a solid triangle. Eight events with $M \geq 4$ locate on this deep reverse fault, for which the inferred downward projection is indicated by a dashed line. Given the relative-location uncertainty, the width of the fault zone imaged by these eight events is not resolvably different from zero. A

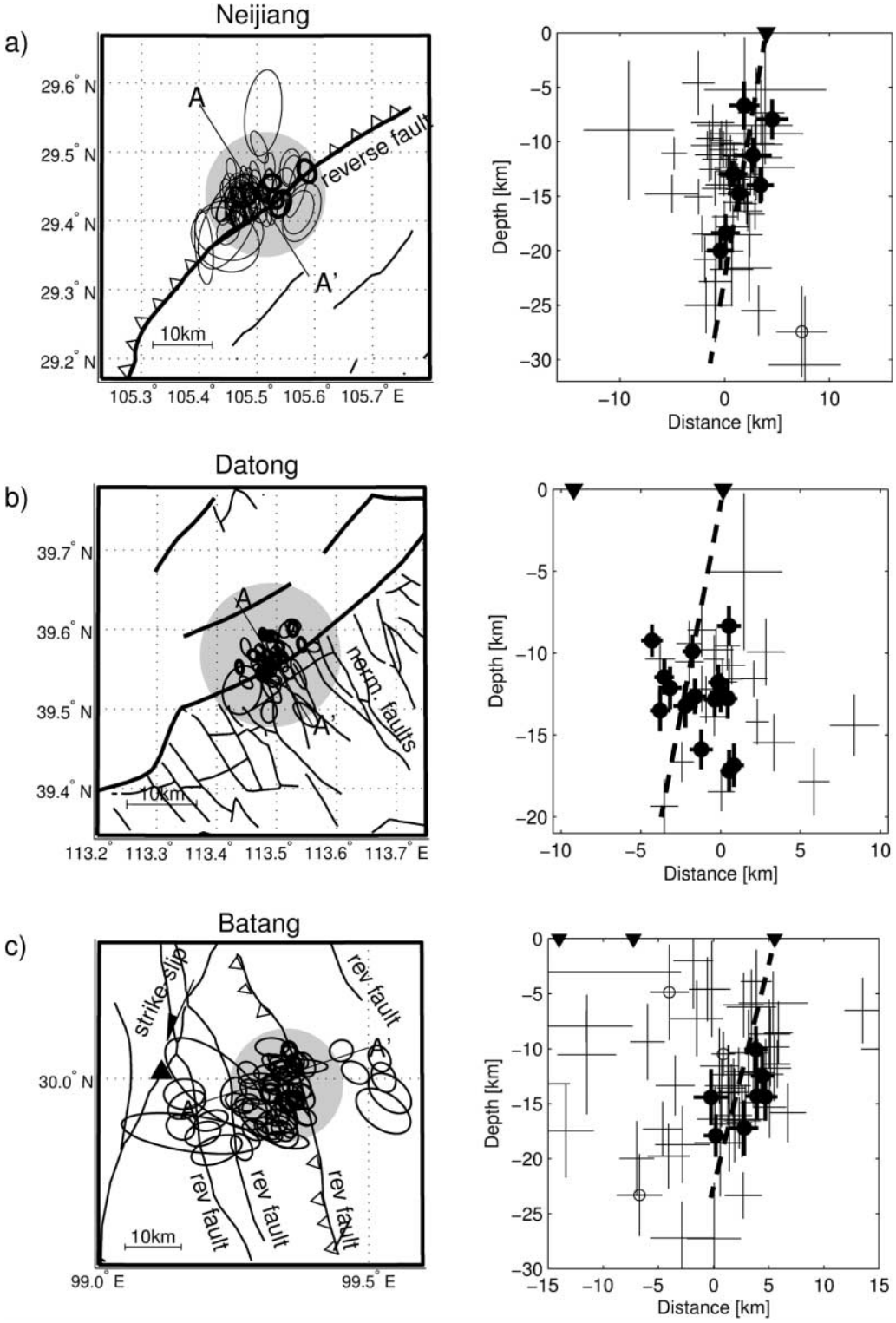


Figure 6. Relocated events in map view (left panel) and fault perpendicular cross section (right panel) along AA′ for events near (a) Neijiang, (b) Datong, (c) Batang, (d) Tangmai, (e) Menyuan, (f) Jinggu. Ellipses (in map view) and crosses (in cross sections) indicate bootstrap errors at the 90% confidence level. Reference events are indicated by thick ellipses or crosses. Lines in map view indicate mapped faults at the surface, and thick lines, those that are described as deep faults in the USGS fault database. Faults are labeled as indicated in the fault database. Triangles denote the projection of the main fault onto the cross section. Dashed line in cross section indicates assumed fault dip based on seismicity. (*continued*)

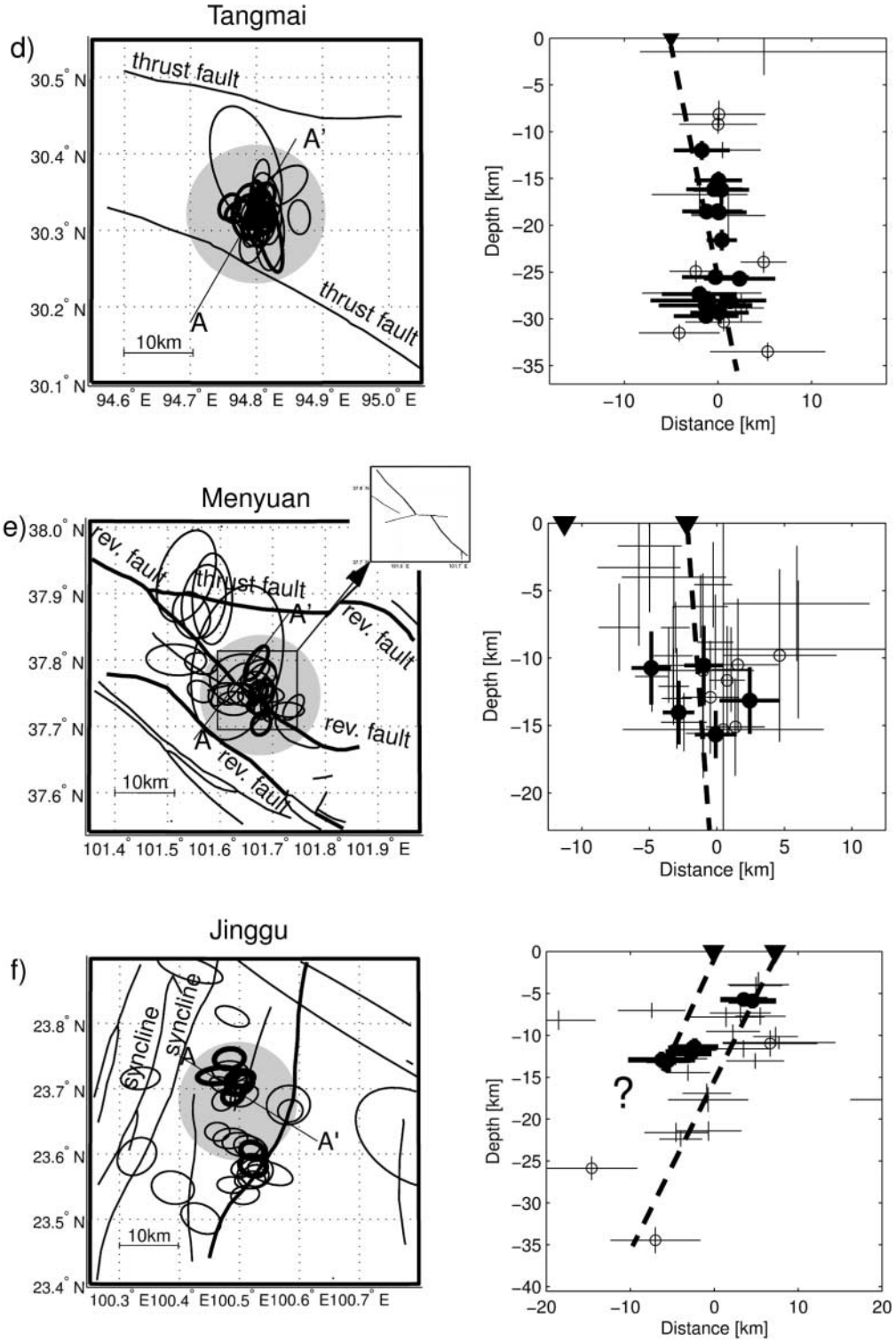


Figure 6. (*continued*). Open circles denote events with $M \geq 3.5$, except in the Batang cluster ($M \geq 5$), and the Tangmai cluster ($M \geq 4.5$). No magnitudes are available for events in the Datong cluster. Gray filled circles in map view are centered on the cluster centroid and indicate the estimated average absolute-location uncertainty associated with the ABCE locations; rev. = reverse; norm. = normal faulting.

Table 4
Reference Events at the GT5 and GT10* Levels

| Date | Time | Lat | Long | Depth | Mag | Location |
|---|---|---|---|---|---|---|
| 1993/08/20 | 06:37:54.64 | 29.440 | 105.485 | 18.4 | 4.5 | Neijiang |
| 1994/04/14 | 17:57:06.24 | 29.441 | 105.511 | 14.7 | 4.4 | Neijiang |
| 1995/12/26 | 03:31:08.15 | 29.456 | 105.526 | 12.9 | 4.2 | Neijiang |
| 1996/01/16 | 00:08:15.86 | 29.408 | 105.467 | 06.7 | 4.2 | Neijiang |
| 1997/02/24 | 18:43:04.24 | 29.431 | 105.532 | 14.0 | 4.5 | Neijiang |
| 1997/08/13 | 08:13:29.83 | 29.473 | 105.587 | 11.2 | 4.8 | Neijiang |
| 1998/02/18 | 06:20:57.43 | 29.435 | 105.469 | 20.0 | 4.0 | Neijiang |
| 1999/08/17 | 10:41:05.03 | 29.425 | 105.541 | 07.9 | 4.8 | Neijiang |
| 1989/10/18 | 15:15:25.37 | 39.566 | 113.486 | 15.9 | – | Datong |
| 1989/10/18 | 17:01:33.24 | 39.568 | 113.463 | 13.2 | – | Datong |
| 1989/10/18 | 18:20:45.88 | 39.553 | 113.438 | 12.6 | – | Datong |
| 1989/10/18 | 19:37:49.36 | 39.592 | 113.486 | 13.5 | – | Datong |
| 1989/10/19 | 10:29:02.53 | 39.594 | 113.478 | 09.2 | – | Datong |
| 1989/10/19 | 12:32:15.66 | 39.544 | 113.474 | 17.2 | – | Datong |
| 1989/10/19 | 13:59:58.90 | 39.592 | 113.494 | 11.5 | – | Datong |
| 1989/10/19 | 17:56:47.80 | 39.579 | 113.505 | 09.9 | – | Datong |
| 1989/10/19 | 23:54:31.48 | 39.601 | 113.528 | 12.1 | – | Datong |
| 1989/10/20 | 11:41:41.62 | 39.581 | 113.542 | 13.0 | – | Datong |
| 1989/10/23 | 13:19:33.14 | 39.567 | 113.510 | 12.8 | – | Datong |
| 1989/10/23 | 17:07:54.28 | 39.557 | 113.488 | 11.8 | – | Datong |
| 1989/10/29 | 02:22:42.85 | 39.548 | 113.482 | 08.3 | – | Datong |
| 1989/12/08 | 13:05:14.00 | 39.549 | 113.484 | 12.8 | – | Datong |
| 1989/12/08 | 23:04:50.84 | 39.543 | 113.477 | 16.8 | – | Datong |
| 1989/12/31 | 08:24:48.13 | 39.559 | 113.499 | 12.4 | – | Datong |
| 1989/04/16 | 18:25:50.26 | 29.977 | 99.319 | 14.4 | 5.1 | Batang |
| 1989/04/25 | 02:13:22.08 | 29.993 | 99.320 | 17.9 | 6.2 | Batang |
| 1989/04/30 | 23:05:26.82 | 29.964 | 99.353 | 17.2 | 5.1 | Batang |
| 1989/05/03 | 05:53:00.94 | 30.020 | 99.362 | 14.4 | 6.1 | Batang |
| 1989/05/03 | 15:41:30.94 | 29.966 | 99.365 | 14.3 | 5.8 | Batang |
| 1989/05/03 | 17:28:21.44 | 30.047 | 99.354 | 12.5 | 5.3 | Batang |
| 1989/05/04 | 05:30:46.27 | 29.963 | 99.364 | 10.1 | 5.1 | Batang |
| 1985/07/18 | 17:40:13.52 | 30.338 | 94.799 | 28.1 | 4.9 | Tangmai* |
| 1985/07/19 | 02:38:08.63 | 30.323 | 94.810 | 16.2 | 4.7 | Tangmai* |
| 1985/07/20 | 18:31:45.12 | 30.319 | 94.818 | 21.6 | 4.6 | Tangmai* |
| 1986/10/10 | 08:59:19.47 | 30.325 | 94.773 | 18.5 | 4.8 | Tangmai* |
| 1986/10/12 | 16:29:11.50 | 30.343 | 94.810 | 25.7 | 4.7 | Tangmai* |
| 1987/09/17 | 01:34:47.20 | 30.330 | 94.788 | 15.2 | 4.9 | Tangmai* |
| 1987/09/19 | 18:59:38.80 | 30.323 | 94.806 | 29.3 | 4.7 | Tangmai* |
| 1991/07/18 | 13:25:00.18 | 30.320 | 94.802 | 25.6 | 5.0 | Tangmai* |
| 1991/07/20 | 18:52:24.44 | 30.309 | 94.802 | 28.6 | 4.5 | Tangmai* |
| 1991/07/20 | 19:02:31.24 | 30.321 | 94.808 | 18.6 | 4.8 | Tangmai* |
| 1991/07/23 | 16:51:53.69 | 30.323 | 94.801 | 18.5 | 4.7 | Tangmai* |
| 1991/07/24 | 06:06:45.16 | 30.306 | 94.794 | 27.4 | 4.8 | Tangmai* |
| 1991/07/25 | 01:52:44.28 | 30.315 | 94.782 | 12.0 | 4.8 | Tangmai* |
| 1991/07/28 | 23:58:20.64 | 30.331 | 94.760 | 29.7 | 4.9 | Tangmai* |
| 1991/07/29 | 03:20:16.09 | 30.305 | 94.816 | 28.1 | 4.6 | Tangmai* |
| 1993/09/06 | 20:57:22.32 | 30.312 | 94.816 | 16.1 | 4.7 | Tangmai* |
| 1986/08/26 | 09:43:00.63 | 37.796 | 101.669 | 13.2 | 6.2 | Menyuan |
| 1986/08/26 | 10:30:00.03 | 37.753 | 101.688 | 15.7 | 5.4 | Menyuan |
| 1986/08/26 | 13:11:24.61 | 37.753 | 101.673 | 10.6 | 5.0 | Menyuan |
| 1986/08/27 | 13:15:23.03 | 37.704 | 101.678 | 10.7 | 4.3 | Menyuan |
| 1987/06/28 | 01:16:36.88 | 37.731 | 101.672 | 14.0 | 4.9 | Menyuan |
| 1993/05/30 | 10:01:10.33 | 23.715 | 100.501 | 11.5 | – | Jinggu* |
| 1993/05/30 | 21:49:02.14 | 23.746 | 100.483 | 13.0 | – | Jinggu* |
| 1993/06/04 | 01:04:00.94 | 23.707 | 100.500 | 11.4 | 4.5 | Jinggu* |
| 1993/06/10 | 20:38:28.68 | 23.691 | 100.490 | 12.2 | 4.6 | Jinggu* |
| 1993/10/25 | 08:32:46.55 | 23.582 | 100.523 | 5.9 | – | Jinggu* |
| 1994/03/18 | 16:16:47.64 | 23.606 | 100.521 | 5.7 | – | Jinggu* |
| 1994/11/07 | 22:40:50.12 | 23.720 | 100.464 | 12.9 | 4.0 | Jinggu* |

ninth $M \geq 4$ event, having larger uncertainty, locates to the southeast away from the fault. Considering the formal uncertainty in relative locations being smaller than 2 km for the eight $M \geq 4$ events, and their correlation with independently mapped surface information, we select these eight larger events as reference events accurate to within 5 km (solid dots in cross section in Fig. 6) (see Table 4 for hypocentral parameters). The positions of the events along the strike of the fault is similar to the locations reported in the printed ABCE for events included in both bulletins (see Fig. 5b). These results are also similar to location results for 20 events derived from a simultaneous inversion of local network data (Z. Yang, personal comm.) for 1D velocity structure and earthquake locations (program VELEST, Roecker, 1977; Kissling et al., 1994).

Figure 6b shows results for the cluster near Datong. This cluster of 42 events was relocated, using a velocity model for the region of northeastern China (Table 3). Most of the events occurred during a swarmlike activity in 1989, including 16 of the largest events (based on the number of stations that recorded them). In map view the cluster of events lines up with a northeast-trending deep fault, southeast and perpendicular to which are a series of northwest-trending normal faults. Parallel to, and about 10 km northwest of, the main fault exists what seems to be a secondary, deep fault. Even though this secondary fault is only 10 km away from the cluster centroid, the complex distribution of the relocated events (no narrow fault zone is imaged) and the indication of seismicity occurring on the normal faults to the southeast lead us to the conclusion that the 16 reference events are associated with the main fault, and stress is transferred to the normal faults that subsequently fail in smaller events.

The 68 events near Batang in Sichuan Province (Fig. 6c) were relocated, using the Sichuan velocity model (Table 3). The closest station, BTA, is only about 20 km away (see triangle in map view of Fig. 6c), but no phase picks are listed in the ABCE bulletin for the events investigated. It is possible, though, that phase picks from this station were used in determining the locations reported in either the electronic or the printed ABCE, but for some reason they are not reported in the bulletins. The relocated events mainly cluster around a north-northwest- striking fault trace that is described as a west-dipping reverse fault. This fault is paralleled by two other reverse faults at some 10-km distance to the southwest and northeast. The reverse faults intersect a left-lateral strike-slip fault to the northwest. None of the faults is labeled as deep, even though the seismicity reaches depths of 25 km. The relocated seismicity correlates well with the fault information at the surface, imaging a west-southwest- dipping fault with an effective width less than 1 km. The seven reference events have magnitudes between 5.1 and 6.2 and are followed by aftershocks, some of which appear to have occurred on the adjacent reverse faults to the northeast and southwest.

Near Tangmai in eastern Tibet, 29 events were relocated using the velocity model for the Tibetan Plateau shown in Table 3. The events locate between two west-northwest-striking thrust faults (Fig. 6d). They image a north-northeast-dipping 35-km-deep structure, a depth not unusual in this part of China. The centroid of the epicenter is within 10-km distance from the thrust fault to the south, but the downward projection of the surface trace is less clear because of the somewhat large horizontal relative errors for the 16 selected reference events, and missing information as to the dip of the fault. Thus we place an upper bound of 10 km to the absolute location uncertainty of these events.

In the Menyuan cluster (Fig. 6e) the relocated seismic activity correlates with a deep northwest-striking reverse fault, right where a small left-lateral stepover configuration exists (see inset in Fig. 6e). We argue that this fault irregularity is the cause of the somewhat complex faulting pattern observed at depth and thus can be used as a benchmark to constrain the absolute location of this cluster. A total of 12 events with $M > 4$ are selected, 5 of which are well constrained and are selected as reference events (Table 4). Additional seismic activity correlates with an adjacent, parallel fault to the southwest, and with a nearby thrust fault northwest of the reference events.

In the Jinggu cluster (Fig. 6f), most of the relocated seismicity appears to occur on a deep fault and possibly on an adjacent, parallel fault to the west, including six of the larger events selected as reference events. The faults are not further specified in the fault database, but the relocated seismicity indicates that they are dipping to the west. A few isolated events seem to occur on additional faults, and some are associated with synclines. Although there is a general agreement between the seismicity and the surface information, the absolute location of the reference events within the tectonic framework given by the limited fault information available to us is not as well constrained as in other clusters. Furthermore, relative-location errors are larger than in most other clusters. We therefore consider these reference events to be within 10 km of the true locations.

## Evaluation of Solution Quality

Several tests were performed to evaluate the stability of the double-difference solutions. In addition to the regional models listed in Table 3, a standard crustal model is used (IASP91) that consists of a 20-km-thick upper crust with a *P*-wave velocity of 5.8 km/sec on top of a 15-km-thick lower crust ($V_p$ = 6.5 km/sec), and an upper-mantle velocity of 8.04 km/sec. Figure 7 compares, for each cluster, the locations of reference events obtained with the regional model (thick black ellipses representing errors at the 90% confidence level, identical to final locations as shown in Fig. 6) with locations from the IASP91 model (thin black ellipses). Note that even though we only show the reference events in Figure 7, all events in a particular cluster are used in the relocation procedure. In general, differences are less than 1 km between the two locations, and error ellipses for locations derived from the IASP91 velocity model are larger

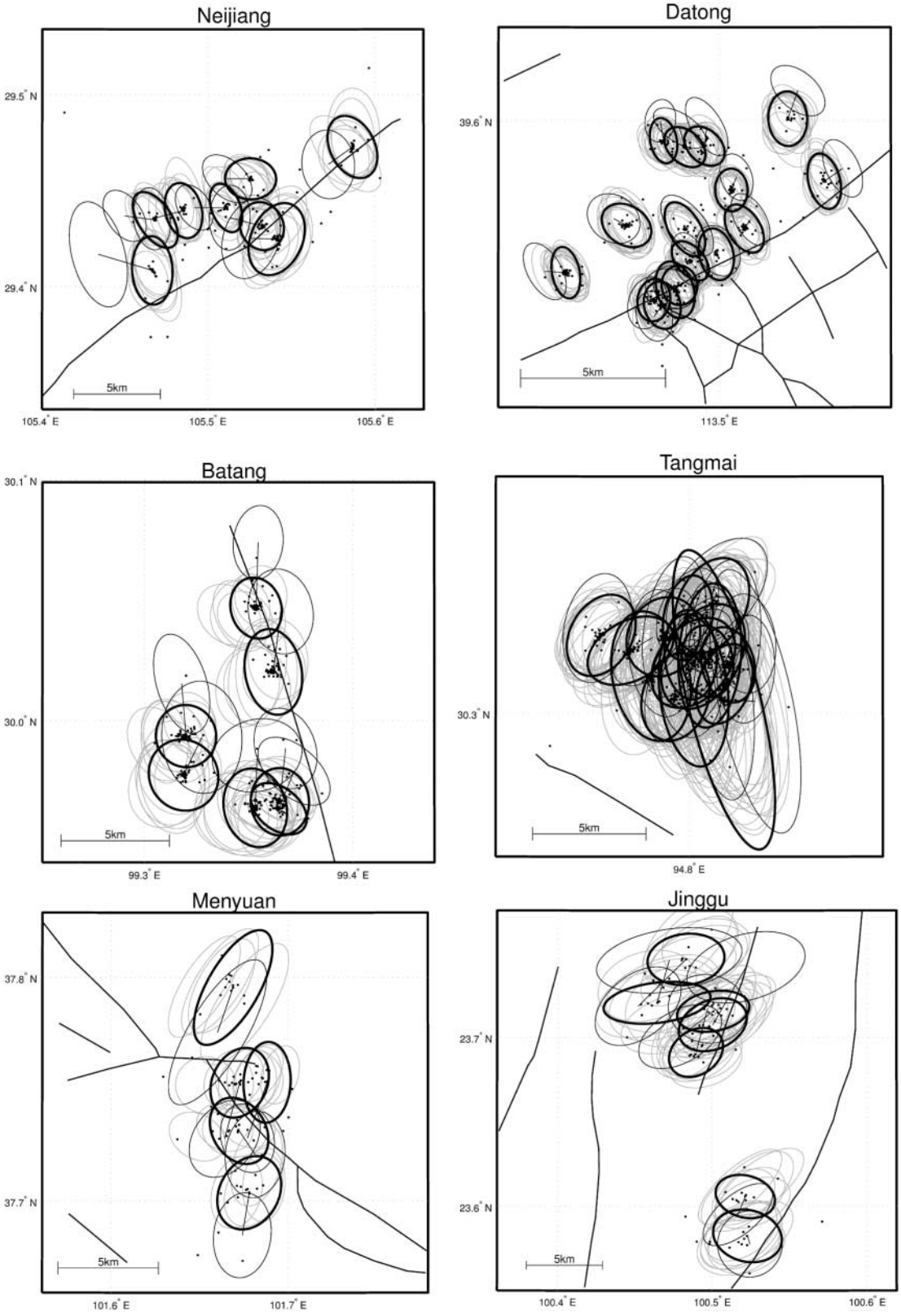


Figure 7. Results from three different tests performed to ensure robustness of the seismicity structure within each cluster. Thick ellipses represent final locations of reference events, thin ellipses show relocation results from using the IASP91 velocity model, gray ellipses are from relocating the events with one event removed at a time, dots are from relocating the events with one station removed at a time. Lines indicate fault traces except for lines that connect the final reference events with locations derived with the IASP91 model. See text for explanation.

than those obtained from the regional models. Error ellipses overlap for corresponding events in almost all cases.

A second test used a jackknife method to investigate the influence of each reference event on the locations of all others. As each event is linked to others through direct measurements, a less-well-constrained event may affect the relative location between others. Each cluster, therefore, was repeatedly relocated with one reference event removed at a time. The results of NEV · (NEV-1) locations are displayed as gray ellipses in Figure 7. The mean in horizontal and vertical deviation of each test location from the event's final location (solid ellipse) is 190 m and 340 m. Error ellipses are similar in most cases.

A third test, again using a jackknife method, assessed the effect of variation in station distribution on event locations. It involved removing one station at a time, each time locating all events within a cluster, using the remaining NSTA-1 stations. The results of NSTA · NEV locations are displayed as dots in each subfigure of Figure 7. The mean deviation of each test location from the centroid of all test locations for a particular event is 200 m in horizontal and 360 m in vertical direction. Ninety-five percent of the 2881 samples are contained within an ellipse that has a major and minor axis of 1.5 and 1 km, respectively. The results from these three tests indicate that changes in the model used to relocate the events, effects from individual reference events on others, and varying station distribution cause changes in relative locations that are generally less than 1 km. In each case the relocated reference events support the characterization of the corresponding faults as indicated in the Chinese fault database.

For some events in the Tangmai and Jinggu clusters, relative-depth errors are smaller than errors in the horizontal directions. The somewhat large horizontal errors are caused by azimuthal gaps in nearby stations (Table 2), whereas relative depths are still well constrained by downgoing ray paths of *Pn* phases observed at greater distances—not that reference events in these two clusters are less well constrained than in the other clusters.

Figure 8 shows absolute travel-time residuals of the 59 reference events observed at the six IMS stations relative to the median travel time for each cluster-station pair, and for double-difference (solid circles) and ABCE (open circles) solutions. Figure 9 indicates the IMS stations that recorded at least one reference event within a particular cluster. A significant reduction in residual scatter is observed, with the standard deviation decreasing from 1.28 sec before to 0.61 sec after relocation. The eight apparent phase-pick outliers (solid squares in Fig. 8) in the Neijiang, Datong, Menyuan, and Jinggu cluster may indicate timing problems. Note that such outliers, determined separately within each cluster, are generally downweighted or removed during the relocation process, and stations other than the affected IMS stations were used to relocate the events. The spread of residuals for events in the Tangmai cluster is larger than in other clusters, with the largest residual being larger than the resiudals of outliers identified in other clusters. This is likely because of the deviation of the true crustal structure from the IASP91 model in the source area, a region of thick lithosphere. The effect of model error is amplified by the large depth extent of the seismic activity to which *Pn* differential travel times are sensitive.

Since we keep the absolute location of the cluster centroid fixed at the initial locations, we are not able to quantify absolute location errors using standard approaches (e.g., by analyzing absolute travel-time residuals), but instead we can validate the absolute location of the clusters and the reference events they include in a tectonic context derived from independent surface information. For comparison of uncertainty estimates based on absolute travel-time residuals relative to the IASP91 travel times, we apply the location procedure *LocSat* (Bratt and Bache, 1988), currently in operation for nuclear-test monitoring at the IDC in Vienna, to the ABCE arrival times of the eight reference events near Neijiang. The resulting errors at the 95% confidence level have major axes ranging from 2.5 to 7.7 km. These major axes are predominantly oriented in a northwest direction perpendicular to the fault, a direction that is well constrained by the combined analysis of relocated seismicity and fault information. Thus we know the absolute locations of these events better than what is possible from the analysis of travel-time residuals alone.

The promotion of seismic reference events to GT5 status (or any other GTn) is based in general on some quantitative measure of the absolute location uncertainty of an event. Bondár *et al.* (2004) proposed, after a thorough investigation of the effect of network geometry on the solution quality of earthquake and explosion locations, that such measures include the characteristics of seismic networks used to locate a particular event. Clearly, the approach followed in this study lacks this type of quantitative measure, because none of the reference events derived here fulfills the GT5 network criteria of Bondár *et al.* (2004), at least not with the stations available to us. On the other hand, one can imagine a case where ground-truth information is available from sources other than seismic data (i.e., surface rupture), providing a reference event at the GT1 level or better, even though stations that might have recorded the event would not meet the particular criteria proposed by Bondár *et al.* (2004).

A subjective component is associated with our procedure in that the relocated seismicity is correlated with (independent) fault information to validate the absolute locations derived from the Chinese bulletins. This makes it difficult to quantitatively estimate the absolute location uncertainty from which to derive the GT level of each reference event. Whereas errors in the relative location of events within each cluster, and errors in the mapping accuracy of the fault traces, are shown to be generally less than 1 km, errors resulting from fault mis-association can be larger. To

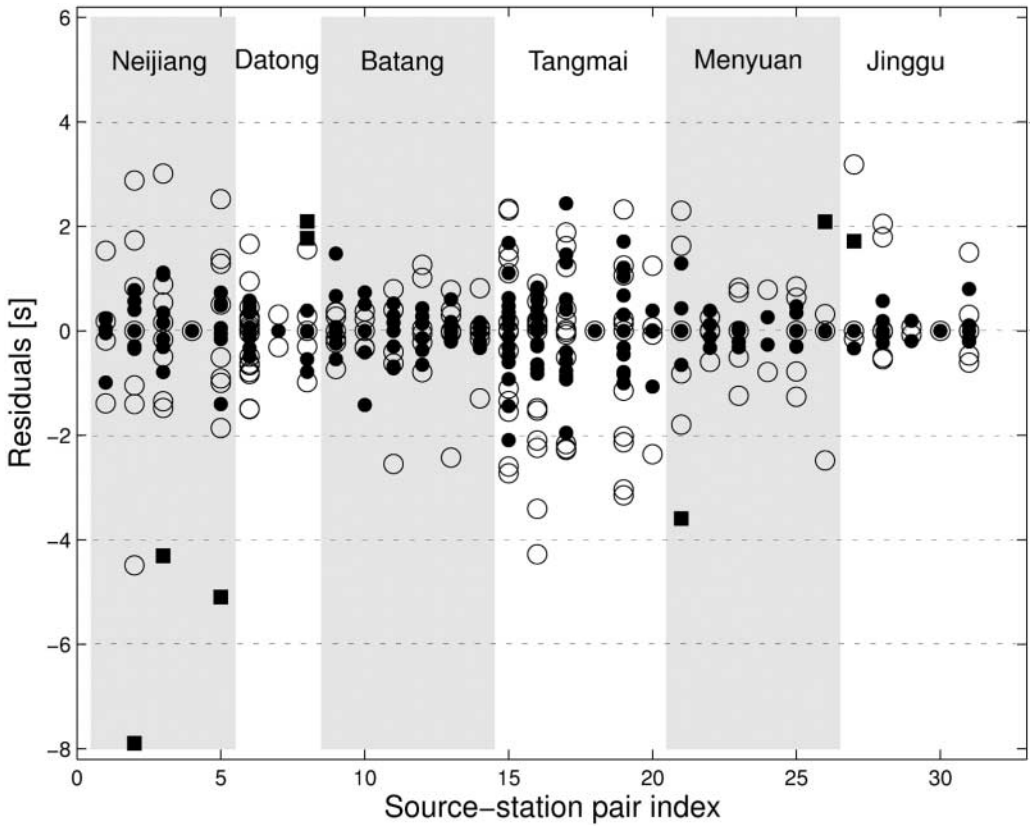


Figure 8. *P*-wave travel-time residuals relative to the median travel time shown for each cluster-station pair (see Fig. 9). Solid circles indicate travel-time residuals from reference events, and open circles, those from the ABCE corresponding locations. Squares indicate phase picks that are considered outliers. Standard deviation for reference-event residuals, after removing the outliers, is 0.61 sec, and for ABCE residuals, 1.28 sec.

estimate upper bounds for these errors, we probe distances out to which a given cluster can be moved without jeopardizing the correlation between seismicity and fault information. For the clusters near Neijiang, Datong, Batang, Menyuan, we find that the relocated seismicity cannot be moved by more than 5 km without causing significant disagreement between the seismicity at depth and the active faulting pattern observed at the surface (Fig. 6 and preceding discussion). For the reference events in the Neijiang cluster, location results using data from a local seismic network limit movement along the strike of the fault to significantly less than 5 km. For the reference events in these four clusters, therefore, we claim that they are accurate to within 5 km, promoting them to GT5 status (Table 4). The reference events in the Tangmai and Jinggu clusters are less accurately determined because of the lower resolution in relative locations and the range of possible correlation with the available fault information. We consider these events accurate to within 10 km, indicating solution qualities at the GT10 level (Table 4). The underlying assumption in assigning these GT levels is that the relocated seismicity actually occurs on the fault we use for validating the absolute locations. In the case of the six clusters of reference events presented here, however, no other mapped fault near the reference events (and within the approximate absolute location uncertainty of the ABCE locations) can likely accommodate several earthquakes of $M \geq 4$.

## Conclusions

The ABCE is used to relocate events in six clusters in central and eastern China to image in detail the active fault at seismogenic depths. The relocated seismicity is associated with fault traces mapped at the surface and related structural information to validate the absolute location of each cluster as derived from the Chinese bulletins. Fifty-nine seismic reference events suitable for calibration of IMS stations in China (and possibly in nearby regions also) are then selected on the basis of event magnitude, relative-location errors, and consistency with the fault information. Substantial reduction in scatter of relative travel-time residuals within each cluster of reference events is achieved, consistent with the relocated

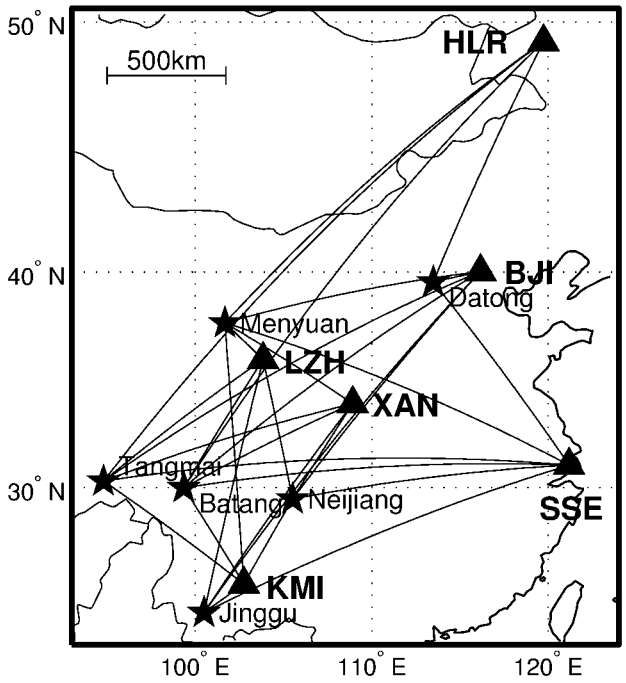


Figure 9. Great-circle paths of *P* waves generated by clustered reference events determined in this study (stars) and recorded at six IMS stations in China (triangles), providing useful calibration data. See Table 1 for station coordinates, and Table 4 for reference-event locations.

positions of these events. Reference events determined in four of the six clusters have solution quality at the GT5 level on the basis of the degree of correlation between seismicity and faulting information. Reference events in the remaining two clusters are at the GT10 level. Each reference event provides *P*- and, in some cases, *S*-phase travel-time information to at least one of six operational or planned IMS stations (Fig. 9).

Prior to this study, reference events for the calibration of IMS stations in China have been derived only from nuclear-explosion data for regions in western China (Fisk, 2002; Waldhauser *et al.*, 2004). Active tectonism from the ongoing collision between India and the Asian continent, however, generates several tens of thousands of earthquakes every year in and near China. Thousands of seismic stations operated by local, provincial, and regional networks record these earthquakes down to low magnitudes. Combining these data across boundaries of individual networks and provinces would substantially increase the density of recorded seismicity across China. The approach outlined here may then be applied on a much larger scale to obtain accurate event locations for entire fault systems, in combination with good information on surface faulting. With about 190 $M \geq 4$ events listed in the ABCE per year, the number of reference events could then be substantially increased. Additionally, accurately located reference events enhance tomographic studies and can improve quantification of seismic hazard.

## Acknowledgments

We are indebted to Chinese seismologists, without whose dedicated work in creating the ABCE this work could not have been carried out. We thank Tom Hearn for his advice on working with ABCE data, Bill Leith for providing us with a copy of the Chinese digital fault map, and Greg Yetman and Francesca Pozzi for their help with reading the GIS format. Reviews by Bob Engdahl and an anonymous reviewer greatly helped to improve the manuscript. This study was supported by Contracts DTRA 01-00-C-0031 of the Defense Threat Reduction Agency and F19268-03-C-0129 of the Air Force Research Laboratory. This is Lamont-Doherty Observatory Contribution Number 6666.

## References

Bondár, I., X. Yang, R. G. North, and C. Romney (2001). Location calibration data for CTBT monitoring at the prototype International Data Center, *Pure Appl. Geophys.* **158,** 19–34.

Bondár, I., S. C. Myers, E. R. Engdahl, and E. A. Bergman (2004). Epicenter accuracy based on seismic network criteria, *Geophys. J. Int.* **156,** 483–496.

Bratt, S., and T. Bache (1988). Locating events with a sparse network of regional arrays, *Bull. Seism. Soc. Am.* **78,** 780–798.

Douglas, A. (1967). Joint epicenter determination, *Nature* **215,** 47–48.

Fisk, M. D. (2002). Accurate locations of nuclear explosions at the Lop Nor test site using alignment of seismograms and IKONOS satellite imagery, *Bull. Seism. Soc. Am.* **92,** 2911–2925.

Hearn, T. M., and J. F. Ni (2001). Tomography and location problems in China using regional travel-time data, in *Proceedings, 23rd Seismic Research Review*, Jackson Hole, Wyoming, Oct. 2–5.

Jih, R. (1998). Location calibration efforts in China, in *Proceedings, 20th Seismic Research Symposium*, Santa Fe, New Mexico, Sept. 21–23.

Jordan, H. T., and K. A. Sverdrup (1981). Teleseismic location techniques and their application to earthquake clusters in the south-central Pacific, *Bull. Seism. Soc. Am.* **71,** 1105–1130.

Kennett, B. L. N., and E. R. Engdahl (1991). Travel times for global earthquake location and phase identification, *Geophys. J. Int.* **105,** 429–465.

Kissling, W., W. L. Ellsworth, D. Eberhard-Phillips, and U. Kradolfer (1994). Initial reference models in local earthquake tomography, *J. Geophys. Res.* **99,** 19,635–19,646.

Murphy, J. R., W. L. Rodi, M. Johnson, J. D. Sultanov, T. J. Bennett, M. N. Töksoz, C. E. Vincent, V. Ovtchinnikov, B. W. Barker, A. M. Rosca, and Y. Shchukin (2002). Seismic calibration of Group 1 International Monitoring System (IMS) stations in eastern Asia for improved event location, in *Proceedings, 24th Seismic Research Review*, Ponte Vedra Beach, Florida, Sept. 17–19.

Ritzwoller, M. H., N. M. Shapiro, A. L. Levshin, E. A. Bergman, and E. R. Engdahl (2003). The ability of a global 3-D model to locate regional events, *J. Geophys. Res.* **108,** no. B7, 2353, ESE 9-1–ESE 9-24.

Roecker, S. W. (1977). Seismicity and tectonics of the Pamir-Hindu Kush region of central Asia, Ph.D. Thesis, Massachusetts Institute of Technology, Cambridge.

Sultanov, D. D., J. R. Murphy, and Kh. D. Rubinstein (1999). A seismic source summary for Soviet peaceful nuclear explosions, *Bull. Seism. Soc. Am.* **89,** 640–647.

Waldhauser, F. (2001). HypoDD: a program to compute double-difference hypocenter locations, *U.S. Geol. Surv. Open-File Rept. 01-113*, Menlo Park, California.

Waldhauser, F., and W. L. Ellsworth (2000). A double-difference earth-

quake location algorithm: method and application to the Northern Hayward Fault, California, *Bull. Seism. Soc. Am.* **90,** 1353–1368.

Waldhauser, F., D. Schaff, P. G. Richards, and W.-Y. Kim (2004). Lop Nor revisited: nuclear explosion locations, 1976–1996, from double-difference analysis of regional and teleseismic data, *Bull. Seism. Soc. Am.* (in press).

Yang, X., I. Bondár, K. McLaughlin, and R. North (2001). Source specific station corrections for regional phases at Fennoscandian stations, *Pure Appl. Geophys.* **158,** 35–57.

Lamont-Doherty Earth Observatory
Columbia University
P.O. Box 1000
Palisades, New York 10964
felixw@ldeo.columbia.edu
(P.G.R., also Department of Earth and Environmental Sciences, Columbia University)

Manuscript received 13 June 2003.